

SURROGATE-BASED OPTIMIZATION OF THE LAYUP OF A LAMINATED COMPOSITE WIND TURBINE BLADE FOR AN IMPROVED POWER COEFFICIENT

DANILO GOMES DELLAROZA, CLAUDIO TAVARES DA SILVA, MARCO ANTONIO LUERSEN

Department of Mechanical Engineering, Federal University of Technology – Parana (UTFPR), Curitiba, Brazil

e-mail: danilodellaroza@gmail.com; tavares@utfpr.edu.br; luersen@utfpr.edu.br (corresponding author)

Most wind turbine blades are made of laminated composite materials. The mechanical properties of the material and the layup orientation influence the blade stiffness and, therefore, turbine performance. The bend-twist coupling effect, a consequence of the stacking sequence, can be used for passive control of the pitch angle, which in turn can improve the turbine performance. In this work, a surrogate-based optimization strategy which uses finite element simulation and radial basis functions is employed to optimize the stacking sequence of the blade laminate of a small wind turbine, aiming to improve the power coefficient.

Keywords: wind turbine blade, laminated composites, optimization, radial basis functions

1. Introduction

Wind turbines convert wind energy into electricity. Aerodynamic forces generate torque on the turbine rotor, and this mechanical power is transformed into electricity by an electric generator. Although most wind turbines consist essentially of the same subsystems, those with lower generating capacity are simpler and do not have active control of the blade angle of attack (see Fig. 1). The ability to control this angle affects turbine performance as it allows the blade to be adjusted according to the wind direction and speed so that the turbine can work close to an optimum position most of the time (Manwell *et al.*, 2009).

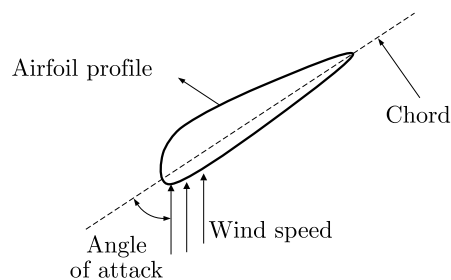


Fig. 1. Representation of a section of a turbine blade

To actively control the angle of attack of the blade, mechanisms and control systems are needed. Because of this, controlling the angle of attack is not feasible in smaller-capacity turbines as it would require most of the energy produced by the turbine. An alternative is to use a bend-twist coupling and perform this control passively, taking advantage of the intrinsic deformation of the turbine blade under aerodynamic loads. The bend-twist coupling is an inherent characteristic of anisotropic materials, such as laminated composites, and can be used for aeroelastic tailoring of wind turbine blades made of composite materials (Veers *et al.*, 1998).

Several studies have evaluated the potential for applying aeroelastic tailoring to wind turbine blades. Veers *et al.* (1998) concluded that aerodynamic loads on a wind turbine blade can be reduced by twisting the blade in the direction that reduces the loads, or towards stall. Although this initially reduces the maximum power generated by the turbine, the reduction in load allows the rotor diameter to be increased, in turn increasing the power over the entire power curve and bringing the maximum power to its original value. The authors concluded that application of aeroelastic tailoring can increase the power generated by a turbine by up to 5% to 10% over a year compared with a turbine with blades made from an isotropic material.

Other authors, such as Maheri *et al.* (2007) and Barr and Jaworski (2019), also obtained improvements in the power curve by applying the same principle as that used by Veers *et al.* (1998). Maheri *et al.* (2007) achieved an increase of around 15.5%, while Barr and Jaworski (2019) reported an increase of 15% in the maximum power generated at certain speeds.

Adopting a different approach, Deilmann (2009) used aeroelastic tailoring to determine the optimum angle of attack regardless of the wind speed to which the turbine is subjected. The analysis was performed for wind speeds of 5 to 11 m/s, and an improvement in power coefficient of up to 6% was achieved. The author concluded that for wind speeds greater than 11 m/s (nominal design wind speed) even greater improvements could be achieved. However, above the nominal design speed an increase in aerodynamic loads is observed, an undesirable effect which can be critical for large turbines.

For all these advantages, the aeroelastic tailoring to be realized requires prior assessment of the behavior of the laminated composite blade. Because evaluation of the design of laminated composite structures is complex and usually has high computational costs, optimization of the design of these structures is usually done with surrogate models (also called metamodels). A metamodel is a simplified surrogate for a detailed model of a phenomenon that has a relatively good accuracy and can therefore be used as a substitute for high-computational-cost functions in the optimization process as it can be evaluated more quickly. Construction of a surrogate model initially requires a design of experiments (DoE) strategy. DoE is a technique that helps to determine values of the design variables used to build the surrogate model (Wang and Shan, 2007).

By combining finite element simulation, DoE, surrogate modeling and optimization algorithm, a design with more efficient, higher-performance laminated structures can be produced. The present work, therefore, intends to develop, apply and evaluate a low-computational-cost optimization methodology to increase the power coefficient of composite wind turbines using radial basis functions (RBFs) as the surrogate model (metamodel).

2. Wind turbine blade optimization procedure

Wang and Shan (2007) proposed a metamodeling-based optimization process that follows the sequence of steps shown in Fig. 2. This sequence is used in the present study to optimize a wind turbine blade. The details of each step are explained in Subsections 2.1 to 2.5.

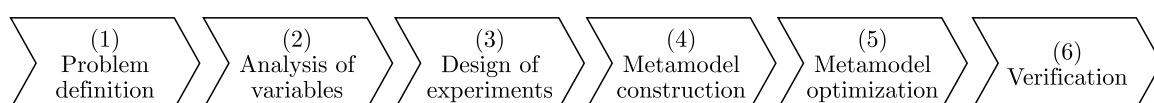


Fig. 2. Flowchart of the metamodeling-based optimization process

2.1. Problem definition

In this work, the wind turbine blade model developed by Leite and Ferreira (2019) is used as the reference, and a corresponding finite element model is generated using Abaqus commercial code. The finite element model is used to simulate torsion generated in the wind turbine blade for different layup configurations. The finite element employed in the numerical model of the blade is the four-node shell (S4R), and static analysis is performed. Newton's method is used to solve the nonlinear system of equations.

Each ply is a unidirectional carbon-epoxy prepreg lamina. The linear elastic regime of the material is considered, but the structure can undergo large displacements (geometric nonlinear analysis). The elastic modulus in the fiber direction E_1 is 121 GPa; the transverse elastic modulus E_2 is 8.6 GPa; the shear modulus in the 1-2 plane G_{12} is 4.7 GPa; and the Poisson ratio in the plane 1-2 ν_{12} is 0.27.

The wind turbine blade is based on the NACA 23018 airfoil. The camber line of the airfoil was used to construct a thin blade on which seven plies of 0.57 mm in thickness were stacked. The orientations of the layers are the input variables for the analysis. The turbine blade has a length of 0.75 m although the useful area starts at a radial distance of 0.15 m. Table 1 shows the chord length and the geometric torsion angle at different radial positions.

Table 1. Geometric characteristics of the wind turbine blade

Radial position [m]	Chord length [m]	Geometric torsion angle [°]
0.15	0.16	20.1
0.20	0.14	14.7
0.26	0.12	10.0
0.32	0.10	6.7
0.38	0.09	4.3
0.45	0.08	2.5
0.51	0.07	1.0
0.57	0.06	-0.1
0.63	0.05	-1.0
0.69	0.05	-1.8
0.75	0.05	-2.5

Two simultaneous loads are applied to the blade. First, a centrifugal load generated by rotation of the blade is applied over the whole airfoil. This load is given by

$$dF_c = dm \Omega^2 r \quad (2.1)$$

where dm is the mass differential, r is the radius and Ω the angular speed, which is given by the following equation proposed by Leite and Ferreira (2019)

$$\Omega = \sqrt{1467.95U + 387.67} - 19.69 \quad (2.2)$$

with U being the wind speed, given in m/s, and Ω given in rad/s.

The second one is the aerodynamic load dF_n , which is obtained using the blade element momentum theory (BEMT). This theory can also be used to calculate the power and efficiency of the turbine. The BEMT is a combination of two different theories: the momentum conservation principle and the blade element theory (Manwell *et al.*, 2009).

The BEMT theory formulates the equations for the torque dQ and thrust dF_n . The wind turbine blade is divided into N sections, and the normal force and torque in each section are given respectively by

$$dF_N = \sigma' \pi \rho \frac{U^2(1-a^2)}{\sin^2 \varphi} (C_l \cos \varphi - C_d \sin \varphi) r \, dr \quad (2.3)$$

and

$$dQ = \sigma' \pi \rho \frac{U^2(1-a^2)}{\sin^2 \varphi} (C_l \cos \varphi - C_d \sin \varphi) r^2 \, dr \quad (2.4)$$

where ρ is density of the fluid, a – axial induction factor, C_l – lift coefficient, C_d – drag coefficient, r – distance from the wind turbine axis and φ is the angle of relative wind. The solidity of the chord σ' is defined as

$$\sigma' = \frac{Bc}{2\pi r'} \quad (2.5)$$

where B is the number of blades and c the chord length (Manwell *et al.*, 2009).

In Eqs. (2.3) and (2.4), the angle φ is directly proportional to the angle of attack, and the variables C_l and C_d are also affected by this angle. Their values are obtained by aerodynamic simulation in open software QBlade and are also affected by the Reynolds number of the flow. Figure 3 shows the finite element model created for the mechanical analysis of the wind turbine blade with its loads and constraints. The mesh has 588 elements, obtained after a convergence test until the difference between displacements of the midpoint of the tip is less than 1% in two consecutive iterations. The aerodynamic load is distributed over the airfoil chord as the equivalent pressure on each finite element in the direction of the wind.

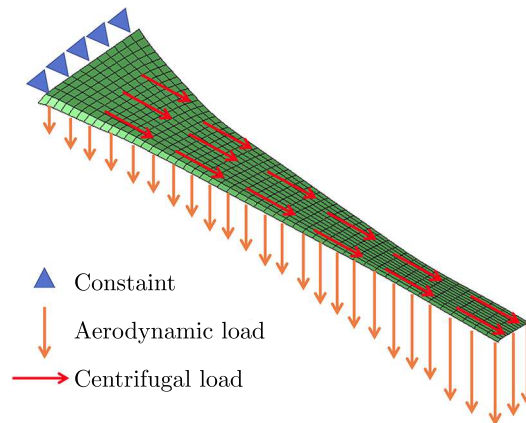


Fig. 3. Loads and constraints of the finite element model

Using BEMT, the turbine power is given by

$$P = \int_r^R \Omega \, dQ \quad (2.6)$$

where r is the internal radius and R the external radius of the wind turbine blade.

Dividing Eq. (2.6) by the power available in the flow gives the power coefficient of the turbine C_p

$$C_p = \frac{P}{P_{flow}} = \frac{\int_r^R \Omega \, dQ}{\frac{1}{2} \rho \pi R^2 U^3} \quad (2.7)$$

According to Betz's law, the maximum possible value for C_p is 0.593 (Almeida, 2009).

2.2. Analysis of variables

Reinforced fiber laminated composite materials are some of the most commonly used materials for wind turbine blades. In these composites, layers with fibers in different orientations are stacked and bonded to each other to give high mechanical strength and stiffness in different directions. A suitable stacking sequence of plies can be selected to obtain the desired properties for a particular application (Reddy, 2003).

The equation that represents how the in-plane loads per unit length \mathbf{N} and moments per unit length \mathbf{M} relate to the in-plane strains $\boldsymbol{\varepsilon}$ and midplane curvature $\boldsymbol{\kappa}$ of a composite laminate is

$$\begin{Bmatrix} \mathbf{N} \\ \mathbf{M} \end{Bmatrix} = \begin{bmatrix} \mathbf{A} & \mathbf{B} \\ \mathbf{B} & \mathbf{D} \end{bmatrix} \begin{Bmatrix} \boldsymbol{\varepsilon} \\ \boldsymbol{\kappa} \end{Bmatrix} \tag{2.8}$$

The submatrices \mathbf{A} , \mathbf{B} and \mathbf{D} form the stiffness matrix of the laminate (the so-called **ABD** matrix). Each term of the matrix represents a deformation mode of the laminate. The matrix terms depend on the elastic properties of plies, their thickness, the number of plies and the stacking sequence (sequence and ply orientation). The main terms associated with bend-twist coupling effects are D_{16} and D_{26} (Reddy, 2003), which affect the aeroelastic tailoring characteristics of the structure.

Thus, for the same loading, each laminate configuration has a unique deformation and, consequently, a different torsion angle. The torsion calculated using the finite element model changes the angle of attack of each wind turbine blade element, which is used to calculate C_p of the turbine. To assess the behavior of the blade over the range of wind speeds to which it will be subjected, the output variable of this study is defined to be the sum of C_p at three different speeds above the nominal design speed of the blade (10 m/s). The wind speeds used to calculate the sum of individual C_p were 13, 15 and 20 m/s. These speeds were used to compose the objective function aiming to achieve an optimal blade design with an improved efficiency for higher wind speeds than the nominal one. These values are chosen to cover a range from a little above the nominal design speed up to the maximum speed of the blade, which is the domain of higher possible gain in power efficiency considering the approach used in this work. Figure 4 depicts the input and output variables of the analysis.

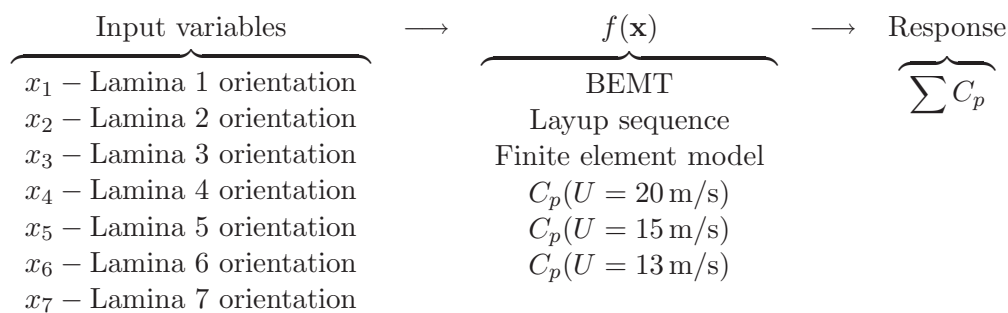


Fig. 4. Objective function and the corresponding input and output variables

Calculation of C_p for each wind speed is an iterative process. First, each wind turbine blade configuration is subjected to the first load, which is calculated based on the non-deformed wind turbine blade. The first load deforms the wind turbine blade, changing the angle of attack and, consequently, the amplitude of this load.

The deformation caused by the loads is determined in the finite element model. Using the deformed blade and the BEMT, a new load is calculated and a new simulation performed. Because each laminate has a different bend-twist coupling effect, each layup will have a different deformation even when subjected to the same load.

This process is repeated until the difference in the displacement at the tip of the blade when the results of two subsequent iterations are compared is less than 1%. When this value is reached, C_p can be calculated for the deformed blade. This sequence is repeated for each wind turbine blade layup sequence for the three wind speeds (13, 15 and 20 m/s).

2.3. Design of experiments (DoE)

The DoE procedure aims to ensure that as much information as possible is obtained using a limited number of experiments. It is also the first step in the construction of the surrogate model and has an influence on the accuracy of the model. In projects where several variables are evaluated and a complex metamodel is constructed, it is recommended that the DoE spreads the design points within the complete design space.

In the Latin hypercube, as in the DoE technique used in this work, each input variable is divided into n non-overlapping intervals of equal probability, where n is the total number of samples desired. A value within each interval is selected randomly. The n values of the first variable are associated with n values of the second variable. These n pairs are randomly combined with n values of the third variable to form n triples, and so on (Myers *et al.*, 2008). In the present work, 15 samples were adopted as the initial set of points.

2.4. Metamodel construction

Several techniques have been developed to create metamodels, including: polynomial regression, Kriging, RBFs, neural networks and support vector regression. With RBFs, the technique adopted here, the surrogate model is built by interpolation of a database of samples \mathbf{x}_i and their responses f_i . The surrogate model is generated by the linear combination of functions centered on the sample point (Lanzi and Giavotto, 2006).

One of the most popular explanation of RBFs is given by Broomhead and Loewe (1998): given a set of n distinct vectors $\{\mathbf{x}_i; i = 1, 2, \dots, n\} \in \mathbb{R}^N$, and n real numbers $\{f_i; i = 1, 2, \dots, n\}$, find a function $s: \mathbb{R}^N \rightarrow \mathbb{R}$ satisfying the conditions

$$s(\mathbf{x}_i) = f_i \quad i = 1, 2, \dots, n \quad (2.9)$$

The RBFs approach introduces a set of n equations that have the form: $\phi(\|\mathbf{x} - \mathbf{x}_i\|)$, where ϕ is some non-linear function (the basis function) which depends on the distance $\|\mathbf{x} - \mathbf{x}_i\|$ and $\mathbf{x} \in \mathbb{R}^N$. The vectors $\mathbf{x}_i \in \mathbb{R}^N$, $i = 1, 2, \dots, n$ are the centers of the RBFs and are obtained from the input database. Therefore, $s(\mathbf{x})$ is given by

$$s(\mathbf{x}) = \sum_{i=1}^n w_i \phi(\|\mathbf{x} - \mathbf{x}_i\|) \quad (2.10)$$

Substituting Eq. (2.10) into conditions (2.9), the following set of linear equations is obtained

$$\begin{Bmatrix} f_1 \\ \vdots \\ f_n \end{Bmatrix} = \begin{bmatrix} A_{11} & \cdots & A_{1n} \\ \vdots & \ddots & \vdots \\ A_{n1} & \cdots & A_{nn} \end{bmatrix} \begin{Bmatrix} w_1 \\ \vdots \\ w_n \end{Bmatrix} \quad (2.11)$$

where

$$A_{ij} = \phi(\|\mathbf{x}_i - \mathbf{x}_j\|) \quad i, j = 1, 2, \dots, n \quad (2.12)$$

Therefore, \mathbf{w} can be obtained by solving the linear system given in (2.11), or, symbolically

$$\mathbf{w} = \mathbf{A}^{-1} \mathbf{f} \quad (2.13)$$

Aiming to generate an RFBs model with improved properties, one of the following parametric basis functions types is usually employed (Forrester *et al.*, 2008):

— Gaussian

$$\phi(r) = e^{-r^2/2\sigma^2} \quad (2.14)$$

— Multiquadratic

$$\phi(r) = \sqrt{r^2 + \sigma^2} \quad (2.15)$$

— Inverse multiquadratic

$$\phi(r) = \frac{1}{\sqrt{r^2 + \sigma^2}} \quad (2.16)$$

where $r = \|\mathbf{x} - \mathbf{x}_i\|$ and σ^2 is the variance. In this study, $\|\cdot\|$ is defined as the Euclidean distance and the Gaussian basis functions are used to build the surrogate model.

2.5. Metamodel optimization and verification

After construction of the surrogate model, new points known as infill points are added in the most promising regions to find the global optimum of the function and thus to improve the accuracy of the surrogate model in these regions. Several methods can be used to determine these additional points. The present work takes advantage of the stochastic refinement method proposed by Regis and Schoemaker (2007), the Global Metric Stochastic Response Surface (G-MSRS). This method is iterative, and at each iteration the surrogate model is updated and a new point selected for the objective function evaluation.

The method requires the following inputs:

- 1) A continuous real-valued function f defined on a compact hypercube $\mathcal{D} = [a, b] \subseteq \mathbb{R}^D$;
- 2) A surrogate model, e.g., RBFs or Kriging (RBFs model is used in the present work);
- 3) A set of n_0 initial evaluation points $\mathcal{J} = [\mathbf{x}_1, \dots, \mathbf{x}_{n_0}] \subseteq \mathcal{D}$ (i.e., the DoE points);
- 4) The number of candidate points in each iteration;
- 5) The maximum number of function evaluations, N_{max} (N_{max} depends on the computational budget/time available).

The output will be the best point reached. The algorithm uses the following steps:

- 1) Evaluate the objective (cost) function at n_0 initial points defined by the DoE (set \mathcal{J}). Set $n = n_0$ and $\mathcal{A}_n = \mathcal{J}$. Consider \mathbf{x}_n^* the point in \mathcal{A}_n with the smallest value;
- 2) While $n < N_{max}$;
 - 2.1) Build/update the surrogate model using the data points $\mathcal{B}_n = \{(\mathbf{x}_i, f_{xi}) : i = 1, \dots, n\}$;
 - 2.2) Randomly generate candidate points $\Omega_n = \{\mathbf{y}_{n,1}, \dots, \mathbf{y}_{n,t}\}$ in \mathbb{R}^d . For each $j = 1, \dots, t$ if $\mathbf{y}_{n,t} \notin \mathcal{D}$ replace $\mathbf{y}_{n,j}$ by the nearest point in \mathcal{D} . The points Ω_n are called the candidate points;
 - 2.3) Considering the surrogate model output and the dataset \mathcal{B}_n , select the next cost function evaluation point \mathbf{x}_{n+1} from the candidate points Ω_n ;
 - 2.4) Evaluate the cost function in \mathbf{x}_{n+1} ;
 - 2.5) Update the information $\mathcal{A}_{n+1} = \mathcal{A}_n \cup \{\mathbf{x}_{n+1}\}$; $\mathcal{B}_{n+1} = \mathcal{B}_n \cup \{\mathbf{x}_{n+1}, f(\mathbf{x}_{n+1})\}$; \mathbf{x}^* is the best point in \mathcal{A}_{n+1} . Return $n = n + 1$;
- 3) Return the best point obtained $\mathbf{x}_{n_{max}}^*$.

Step 2.2 was implemented such that the convergence requirements stated in Regis and Schoemaker (2007) were satisfied. These include ensuring: (i) that the random candidate points are all contained in \mathcal{D} and that two sample sets are generated in this step; (ii) that the first set has points uniformly distributed over the domain; (iii) and that the second set is generated by random perturbation of the best point x^* obtained so far.

In step 2.3, selection of the next evaluation point is based on two criteria: the estimated value of the function calculated by the surrogate model and the distance from points already evaluated. Each candidate point generated in step 2.2 is given a score between 0 and 1 based on the two criteria. A more desirable point receives a score closer to 0. As the objective is to minimize the cost function and evaluate the greatest number of candidate points, a good candidate point will have a low cost function value and can be far from the points previously evaluated \mathcal{A}_n . The next cost function evaluation point is the one that has the lowest score of all the candidate points. Step 2.3 can be divided as follows:

- a) For each $\mathbf{x} \in \Omega_n$ compute the result from the surrogate model $s_n(\mathbf{x})$;
- b) For each $\mathbf{x} \in \Omega_n$ compute the minimum distance from the previously evaluated points $\Delta_n(\mathbf{x}) = \min_{1 \leq i \leq n} D(\mathbf{x}, \mathbf{x}_i)$;
- c) For each $\mathbf{x} \in \Omega_n$ compute $V_n^R(\mathbf{x}) = (s_n(\mathbf{x}) - s_n^{\min}) / (s_n^{\max} - s_n^{\min})$;
- d) For each $\mathbf{x} \in \Omega_n$ compute $V_n^D(\mathbf{x}) = (\Delta_n^{\max} - \Delta_n(\mathbf{x})) / (\Delta_n^{\max} - \Delta_n^{\min})$;
- e) For each $\mathbf{x} \in \Omega_n$ compute $W_n(\mathbf{x}) = w_n^R V_n^R(\mathbf{x}) + w_n^D V_n^D(\mathbf{x})$;
- f) Select the next evaluation point for the cost function \mathbf{x}_{n+1} that minimizes the function W_n .

In order to guarantee convergence to the global minimum of the function, Mueller (2012) proposes that the weights of the parameters, the distance from points previously evaluated and the response from the surrogate model be varied at each iteration. The proposal can be formulated as follows:

As w_n^D and w_n^R are nonnegative weights to balance global and local searches such that $w_n^D + w_n^R = 1$, let $w_n^D = 1$ and at each subsequent iteration subtract 0.1 from this parameter until $w_n^D = 0$. Afterwards, the value of w_n^D is reset to 1 and a new cycle starts. This process is repeated until the maximum number of cost function evaluations is reached.

3. Results and discussion

Combined application of the techniques described in Section 2 allows a layup sequence for a wind turbine blade with an optimal power coefficient to be obtained. Figure 5 shows the result of the objective function for each iteration. The first 15 responses are obtained by simulation of the samples generated by the DoE. The rest of the responses are the results of the sequential refinement. The best value of the objective function during the DoE is 1.511. In the sequential refinement and optimization phase, the maximum value after 27 iterations is 1.522.

In order to determine the accuracy of the surrogate model, the difference between the value predicted by the metamodel and the observed value in each iteration of the sequential refinement phase is calculated (see Fig. 6). Not only the absolute errors are very close to zero, but the proportional mean error of the iterations is 0.31%, indicating that the surrogate model is very accurate.

The mean square error is also evaluated and converges to 0.00004 after 27 iterations, as shown in Fig. 7. However, this convergence is not confirmed in additional iterations, and the mean square error oscillates as new simulations are added. This behavior is caused by the sequential refinement, which starts a new search for the optimum in a little-explored region every 10 iterations, as proposed by Mueller (2012).

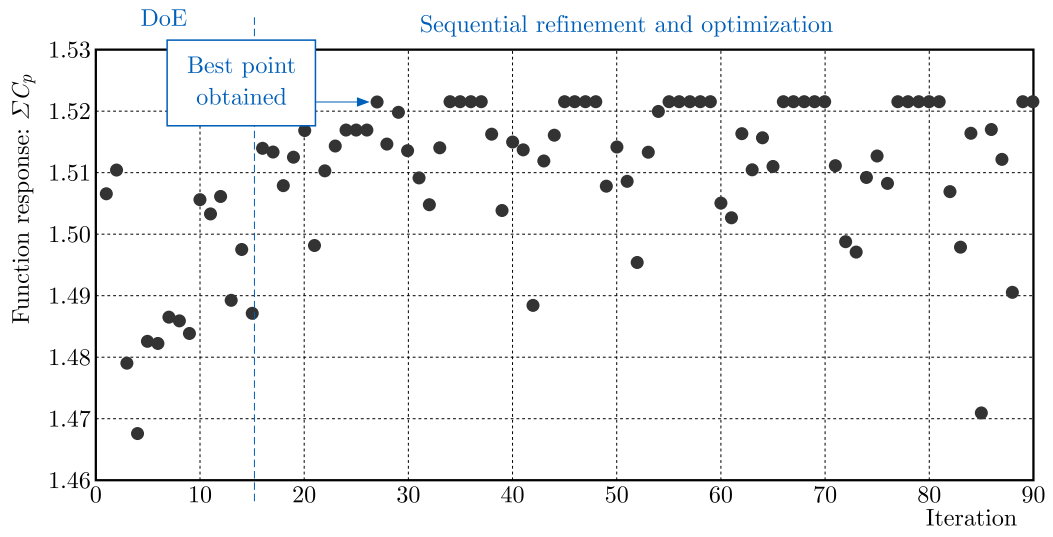


Fig. 5. Response of the objective function in each iteration

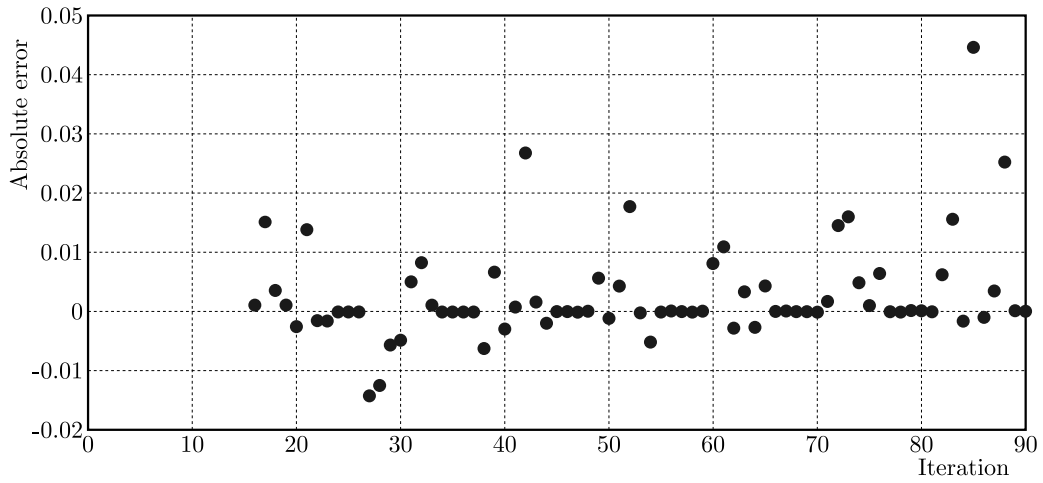


Fig. 6. Absolute error per iteration

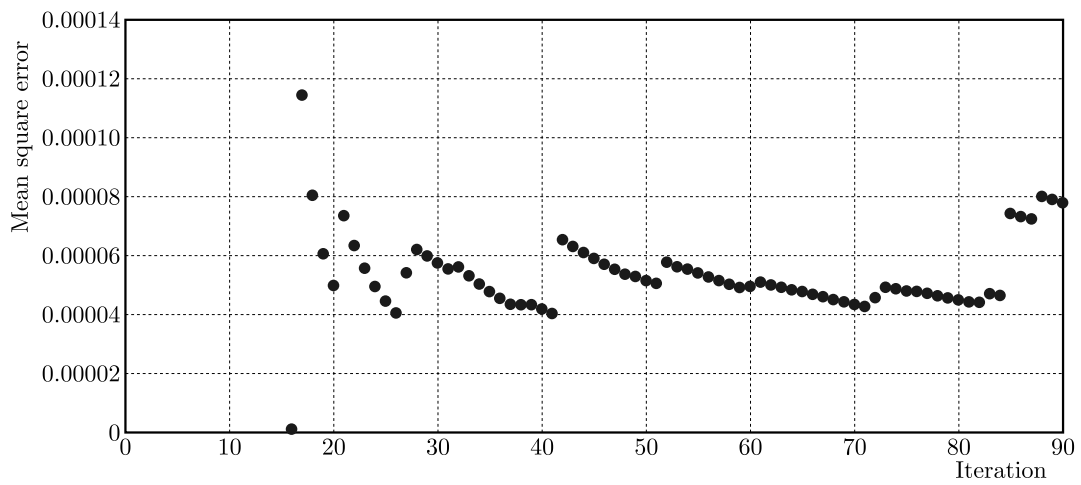


Fig. 7. Absolute error per iteration

As the new iterations are added, the amplitude of these oscillations should decrease until some point when they are no longer noticeable. When this point is reached, there is nothing to be gained from adding the new responses from the cost function to the surrogate model. However, this number of iterations was not reached in the present study, which sought for the optimum using less than 90 cost function responses.

The speed and accuracy with which an RBFs surrogate model can optimize composite structures was also investigated in studies by Lanzi and Giavotto (2006) and Nik *et al.* (2014). In those analyses, the authors noted that structural problems associated with laminated composite structures could be represented with a high degree of reliability using RBFs.

The results of the present study also show the efficiency of the sequential refinement and optimization technique proposed by Regis and Schoemaker (2007) for optimization of laminated composite structures as the optimal result was obtained after 27 iterations (or evaluations of the cost function).

In order to evaluate its efficiency and ensure that the benefits it affords can be observed, the proposed methodology is applied three times consecutively to the problem in question, and each time a new set of starting points (DoE) is generated. Although the mean improvement compared with the best value for the DoE was small (0.6%), this value is merely representative because it evaluates the sum of C_p at only three different speeds.

To evaluate the real gain in the power generated, the laminate configurations that had the highest and lowest values of $\sum C_p$ were selected, i.e., laminate 1 and laminate 2, respectively. It is clear from the C_p curves for these laminates, which are shown in Fig. 8, that a correct use of aeroelastic tailoring can bring considerable gains in the design of laminated wind turbine blades for wind speeds above the nominal design speed (10 m/s). For a wind speed of 13 m/s, the difference can be as much as 2.1%, while at a wind speed of 15 m/s the difference is 3.1% and for a wind speed of 20 m/s the difference between the laminates can be as high as 8.4%. These results provide ample justification for the development and use of a methodology that speeds up the optimization of the design of composite wind turbine blades.

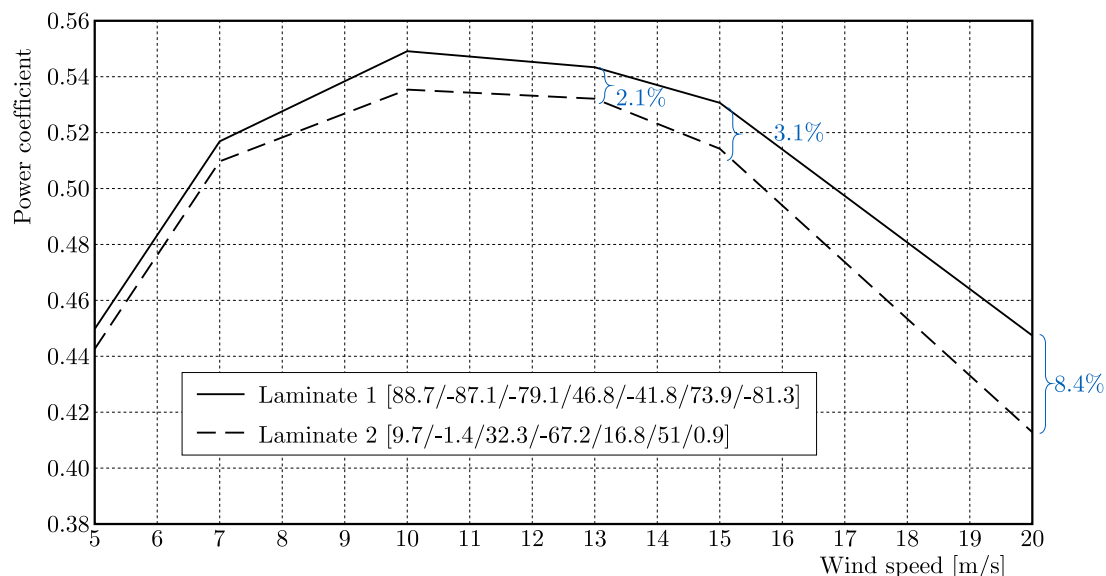


Fig. 8. C_p vs. wind speed curves for the best and worst laminate configurations

The increase in the power coefficient is made by merely redefining the layup sequence. No investments in the manufacturing process are needed and no additional costs are incurred. All that is needed is to adjust the manufacturing process.

The increase in the power coefficient obtained using aeroelastic tailoring corroborates the results reported by Veers *et al.* (1998), Maheri *et al.* (2007) and Barr and Jaworski (2019), who achieved gains of up to 15% in some regions of the turbine operating range. Although these three works, like the present study, used aeroelastic tailoring, they adopted a different approach to that used here and sought for reduction of the maximum load by passive control in order to increase the diameter of the rotor, thereby increasing the power generated. Using an approach similar to that described here, Deilmann (2009) used aeroelastic tailoring to ensure that the blades always operated with the highest lift coefficient and lowest drag coefficient, thereby generating a greater torque than an isotropic blade and increasing the power generated. The analysis carried out by Deilmann (2009) indicated a performance increase of 6%.

Figures 9 and 10 show the variation of the lift and drag coefficients, respectively, over the span of the blade for laminates 1 and 2, considering a wind speed of 20 m/s. From these figures, it can be clearly observed that laminate 1 generates a greater torque in the turbine than laminate 2, and in which position the gain is higher.

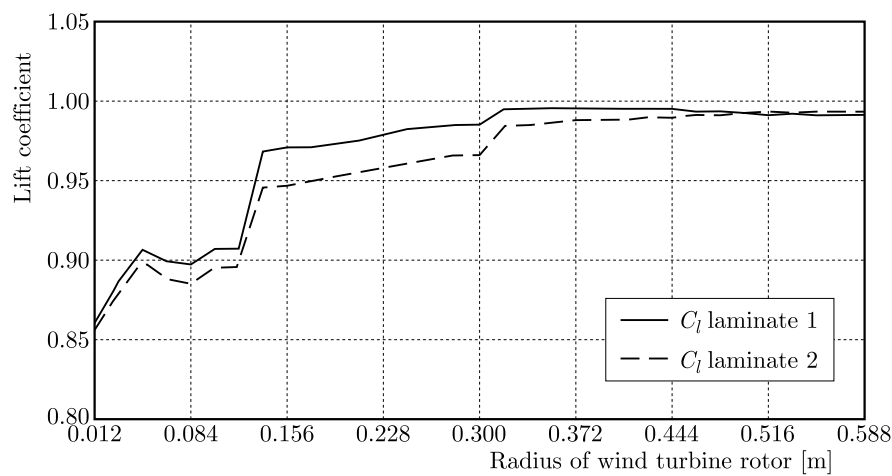


Fig. 9. Lift coefficient vs. radius of the wind turbine blade for laminates 1 and 2

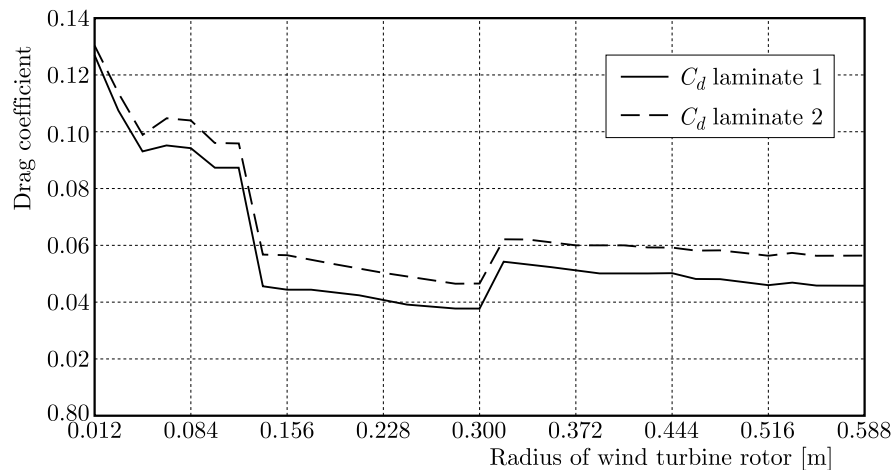


Fig. 10. Drag coefficient vs. radius of the wind turbine blade for laminates 1 and 2

Comparison of the power gain for laminate 1 in relation to laminate 2 shows that this follows the difference in C_p for the two laminates, which increases as the wind speed increases above the nominal design speed. Figure 11 shows these differences in the power curves at wind speeds greater than 13 m/s, a speed at which a significant increase in power begins to be observed.

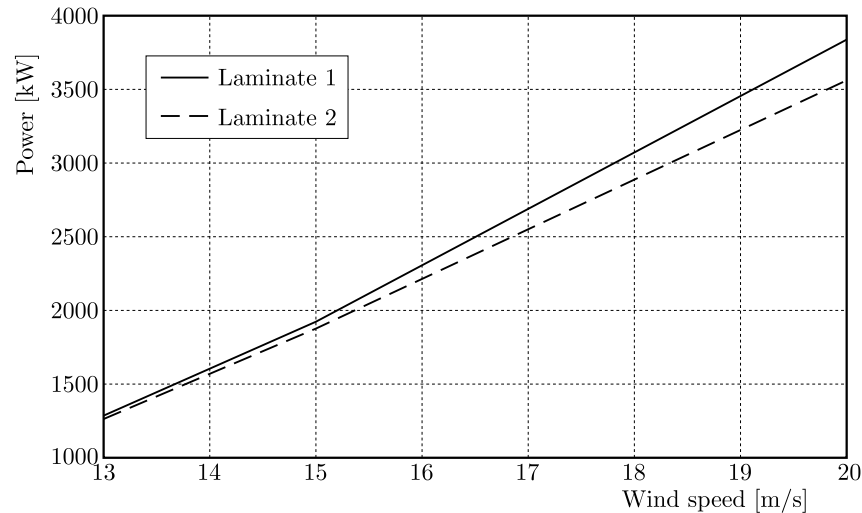


Fig. 11. Power generated by laminates 1 and 2 vs. wind speed

Use of passive adaptation at wind speeds greater than the nominal design speed, as proposed here, has an undesirable effect: an increased load on the blade. Comparison of the results for laminates 1 and 2 shows that there is an increase of up to 1.7 Nm in the torque and up to 0.8 Nm in the normal force when laminate 1 is used for the turbine blade. Although the absolute numbers are relatively small and may be of no practical consequence, structural verification with a more detailed numerical model is recommended.

As already mentioned, one of the issues in any evaluation of a wind turbine blade is the computational effort needed. In this work, evaluation of each laminate configuration takes around 5 minutes. This includes the whole calculation process, from structural simulation to calculation of C_p with all necessary iterations. The computer used has an Intel Core i5 processor running at 2.5 GHz and 8 GB of RAM.

The total number of input variables is seven, corresponding to the orientations of the laminate in each layup. As the orientation can vary from -90° to $+90^\circ$, millions of combinations of layups are possible. Investigation of all these configurations would take an extremely long time.

The methodology proposed here identified the optimal stacking sequence after 27 iterations, or approximately 2 hours of computer processing, indicating that there is a need for continued development of faster methods for evaluating wind turbine blade designs. When combined with optimization methods, surrogate models yield satisfactory results and can go some way to addressing this problem.

4. Concluding remarks

The methodology proposed by Wang and Shan (2007) was adapted here and used to optimize the layup sequence of a composite wind turbine blade. The results were considered satisfactory. One of the main issues when optimizing the layup sequence of wind turbine blades is the high computational cost. However, the proposed methodology appears to have overcome this issue as it allowed the optimal sequence to be identified after about 27 computational experiments (simulations).

The surrogate approach based on RBFs used here proved to be quite a suitable method for this application as it predicted the results of the high-fidelity model (i.e., the finite element model) over the entire domain.

Finally, it was found that the use of aeroelastic tailoring could generate C_p gains at wind speeds higher than the nominal design speed. The gain in C_p for laminate 1 in relation to laminate 2 increases continuously as the wind speed increases, and at higher wind speeds the

difference between C_p for an aeroelastically tailored wind turbine blade and C_p for a blade with an inefficient layup sequence can be as much as 8.4%.

The approach to aeroelastic tailoring proposed here appears to be better suited to small wind turbines, where the loads are not so critical. For large wind turbines, it may be more appropriate to use aeroelastic tailoring and active control together as the former can reduce the loads so that the overall active and passive control is more efficient, as proposed in some studies.

References

1. ALMEIDA M.S., 2013, Computational implementation for the development of horizontal axis wind turbine blades (in Portuguese), Master's Dissertation, Federal University of Ceará, Brazil
2. BARR S.M., JAWORSKI J.W., 2019, Optimization of tow-steered composite wind turbine blades for static aeroelastic performance, *Renewable Energy*, **139**, 859-872
3. BROOMHEAD D.S., LOEWE D., 1988, Multivariate functional interpolation and adaptive networks, *Complex Systems*, **2**, 3, 321-355
4. DEILMANN C., 2009, Passive aeroelastic tailoring of wind turbine blades – a numerical analysis, Master's Dissertation, Massachusetts Institute of Technology, USA
5. FORRESTER A.I.J., SÓBESTER A., KEANE A.J., 2008, *Engineering Design via Surrogate Modelling: A Practical Guide*, John Wiley & Sons, India
6. LANZI L., GIAVOTTO V., 2006, Post-buckling optimization of composite stiffened panels: Computations and experiments, *Composite Structures*, **73**, 2, 208-220
7. LEITE I.T., FERREIRA J.V., 2019, Proof of concept of passive twist angle control in small wind turbines (in Portuguese), Undergraduate Final Project, Federal University of Technology – Parana, Brazil
8. MAHERI A., NOROOZI S., VINNEY J., 2007, Application of combined analytical/FEA coupled aero-structure simulation in design of wind turbine adaptive blades, *Renewable Energy*, **32**, 12, 2011-2018
9. MANWELL J.F., MCGOWAN J.G., ROGERS A.L., 2009, *Aerodynamics of Wind Turbines, Wind Energy Explained: Theory, Design and Application*, John Wiley & Sons Ltd., UK 10
10. MUELLER J., 2012, Surrogate model algorithms for computationally expensive black-box global optimization problems, Doctoral Thesis, Tampere University of Technology, UK
11. MYERS R.H., MONTGOMERY D.C., ANDERSSON-COOK C.M., 2008, *Experimental Designs for Fitting Response Surfaces, Response Surface Methodology: Process and Product Optimization Using Designed Experiments*, John Wiley & Sons, New Jersey, USA
12. NIK M.A., FAYAZBAKSH K., PASINI D., LESSARD L., 2014, A comparative study of metamodelling methods for the design optimization of variable stiffness composites, *Composite Structures*, **107**, 494-501
13. REDDY J.N., 2003, *Mechanics of Laminated Composite Plates and Shells: Theory and Analysis*, Boca Raton, USA
14. REGIS R.G., SCHOEMAKER C.A., 2007, A stochastic radial basis function method for the global optimization of expensive functions, *INFORMS Journal on Computing*, **19**, 4, 497-509
15. VEERS P., LOBITZ D., BIR G., 1998, Aeroelastic tailoring in wind-turbine blade applications, Windpower'98, *American Wind Energy Association Meeting and Exhibition*, Bakersfield, California, USA
16. WANG G., SHAN S., 2007, Review of metamodeling techniques in support of engineering design optimization, *Journal of Mechanical Design*, **129**, 4, 370-380